

## PERLE – BEAM OPTICS DESIGN\*

S.A. Bogacz, Jefferson Lab, Newport News, VA, USA

### Abstract

PERLE (Powerful ERL for Experiments) [1] is a novel ERL test facility, initially proposed to validate design choices for a 60 GeV ERL needed for a future extension of the LHC towards a hadron-electron collider, the LHeC [2]. Its main goal is to test the limits of a high current, CW, multi-pass operation with superconducting cavities at 802 MHz (and perhaps exploring other frequencies of interest). PERLE optics features Flexible Momentum Compaction (FMC) lattice architecture for six vertically stacked return arcs and a high current, 5 MeV photo-injector. With only one pair of 4-cavity cryomodules, 400 MeV beam energy can be reached in three re-circulation passes, with beam currents in excess of 15 mA. This unique quality beam is intended to perform a number of experiments in different fields reaching from uncharted tests of accelerator components via elastic ep scattering to laser-Compton backscattering for photon physics [3]. Following the experiment, the CW beam is decelerated in three consecutive passes back to the injection energy, transferring virtually stored energy back to the RF.

### LAYOUT AND ENERGY

PERLE accelerator complex is arranged in a racetrack configuration; hosting two cryomodules (containing four, 5-cell, cavities operating at 802 MHz), each located in one

of two parallel straights, completed with a vertical stack of three recirculating arcs on each side. The straights are about 10 meter long and the 180° arcs are 5.5 meter across. Additional space is taken by 4 meter long spreaders / recombiners, including matching sections. As illustrated in Fig. 1, the total ‘footprint’ of PERLE is: 24 m × 5.5 m × 0.8 m; the last dimension reflecting 40 cm vertical separation between the arcs. Each of the two cryomodules provides 65.5 MeV energy boost. Therefore, in three turns, a 393 MeV energy increase is achieved. Adding initial injection energy of 5 MeV yields the total energy of 398 MeV – call it ‘400 MeV’.

### MULTI-PASS LINAC OPTICS WITH ENERGY RECOVERY

Multi-pass energy recovery in a racetrack topology explicitly requires that both the accelerating and the decelerating beams share the individual return arcs. This in turn, imposes specific requirements for the TWISS function at the linacs ends: the TWISS functions have to be identical for both the accelerating and decelerating linac passes converging to the same energy and therefore entering the same arc.

To represent beta functions for multiple accelerating and decelerating passes through a given linac, it is convenient to reverse the linac direction for all decelerating passes and string them together with the interleaved accelerating passes, as illustrated in Fig. 2. This way, the corresponding

\* Work has been authored by Jefferson Science Associates, LLC under Contract No. DE-AC05-06OR23177 with the U.S. Department of Energy.

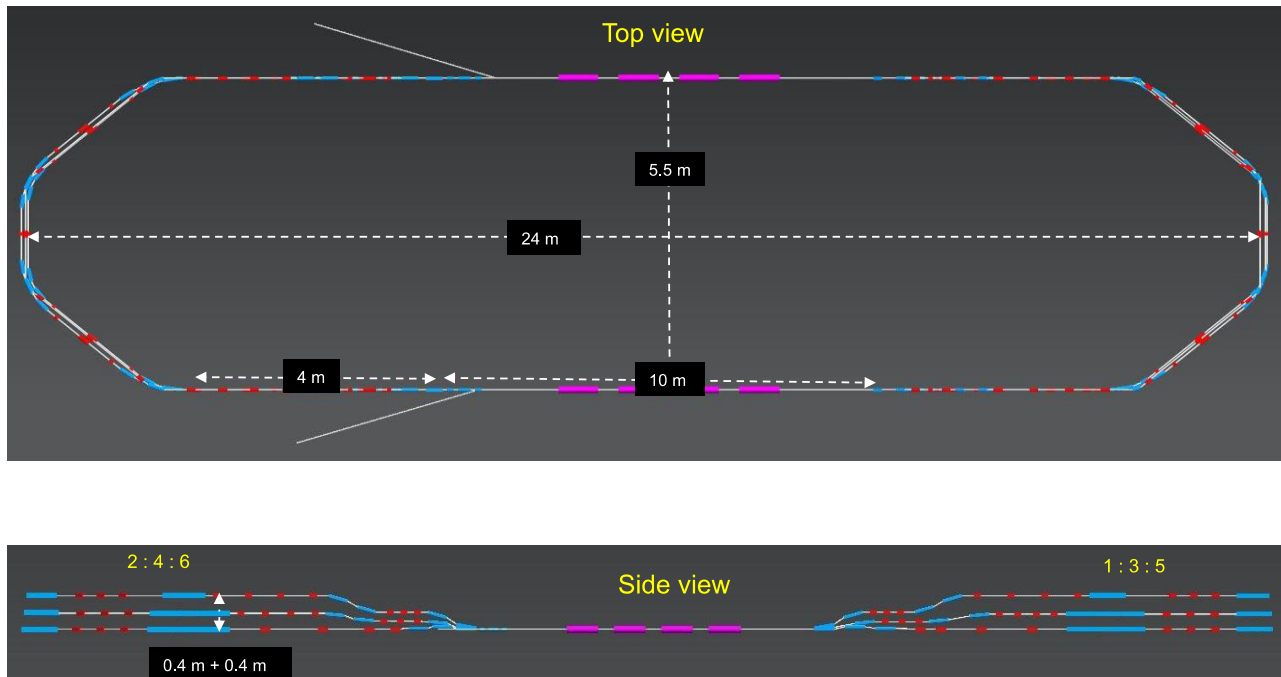


Figure 1: PERLE layout featuring two parallel linacs each hosting a 65.5 MeV cryomodule, achieving 400 MeV in three passes.

Content from this work may be used under the terms of the CC BY 3.0 licence (© 2018). Any distribution of this work must maintain attribution to the author(s), title of the work, publisher, and DOI.

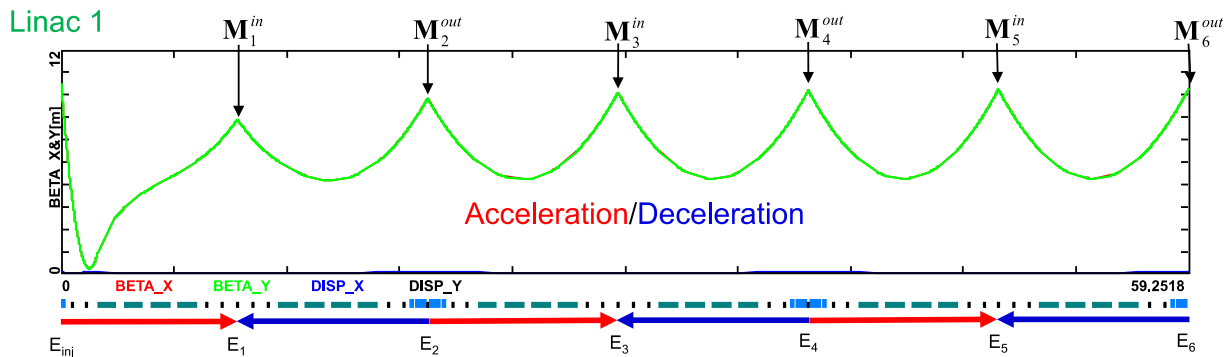


Figure 2: Multi-pass linac optics. Green curve illustrates symmetrically optimized beta functions across different passes through the linac; Red/Blue arrows indicate the accelerating/decelerating passes.

accelerating and decelerating passes are joined together at the arcs entrance/exit, automatically satisfying the matching conditions into the arcs.

Injection at 5 MeV into the first linac is done through a fixed field injection chicane, with its last magnet (closing the chicane) being placed at the beginning of the linac. It closes the orbit ‘bump’ at the lowest energy, injection pass, but the magnet (physically located in the linac) will deflect the beam on all subsequent linac passes. In order to close the resulting higher pass ‘bumps’, the so-called reinjection chicane is instrumented, by placing two additional opposing bends in front of the last chicane magnet. This way, the re-injection chicane magnets are only ‘visible’ by the higher pass beams.

The second linac in the racetrack is configured exactly as a mirror image of the first one, with a replica of the re-injection chicane at its end, which facilitates a fixed-field extraction of energy recovered beam to the dump (at 5 MeV).

## RECIRCULATING ARC ARCHITECTURE

The spreaders are placed directly after each linac to separate beams of different energies and to route them to the

scorresponding arcs. The recombiners facilitate just the opposite: merging the beams of different energies into the same trajectory before entering the next linac.

As illustrated in Fig. 3, each spreader starts with a vertical bending magnet, common for all three beams, that initiates the separation. The highest energy, at the bottom, is brought back to the initial linac level with a chicane. The lower energies are captured with a two-step vertical beamline. The vertical dispersion introduced by the first step bends is suppressed by the three quadrupoles located appropriately between the two steps. The lowest energy spreader is configured with three curved bends following the common magnet, because of a large bending angle (45°) the spreader is configured with. This minimizes adverse effects of strong edge focusing on dispersion suppression for a lower energy spreader. Following the spreader, there are four matching quads to ‘bridge’ the TWISS function between the spreader and the following 180° arc (two betas and two alphas).

All six, 180° horizontal arcs are configured with the FMC optics to ease individual adjustment of  $M_{56}$  in each arc (needed for the longitudinal phase-space re-shaping, essential for operation with energy recovery). The lower

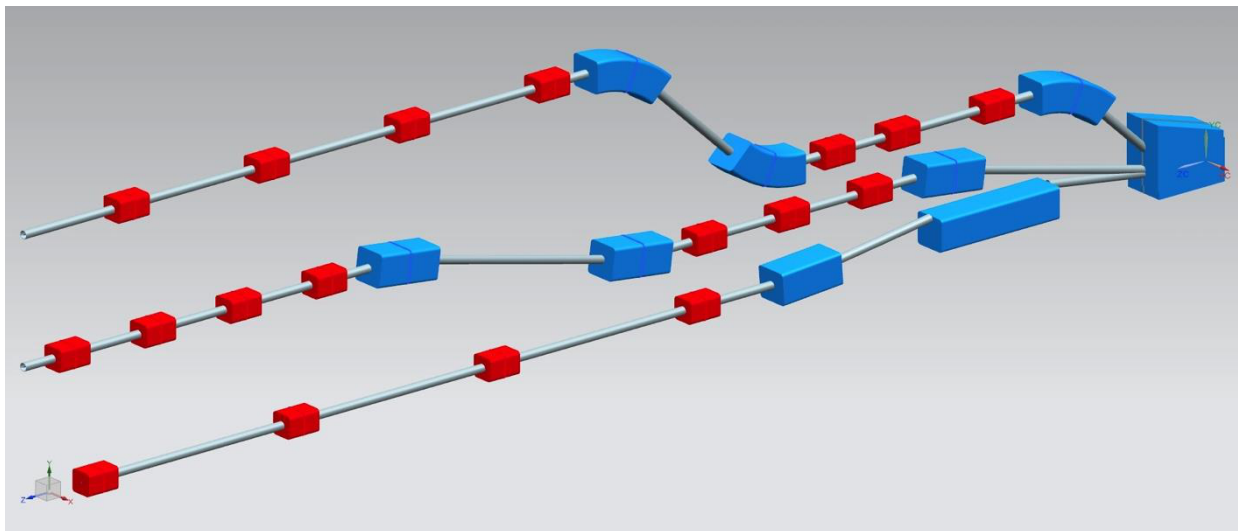


Figure 3: Layout of a three-beam switchyard with the corresponding energy ratios: 1:3:5.

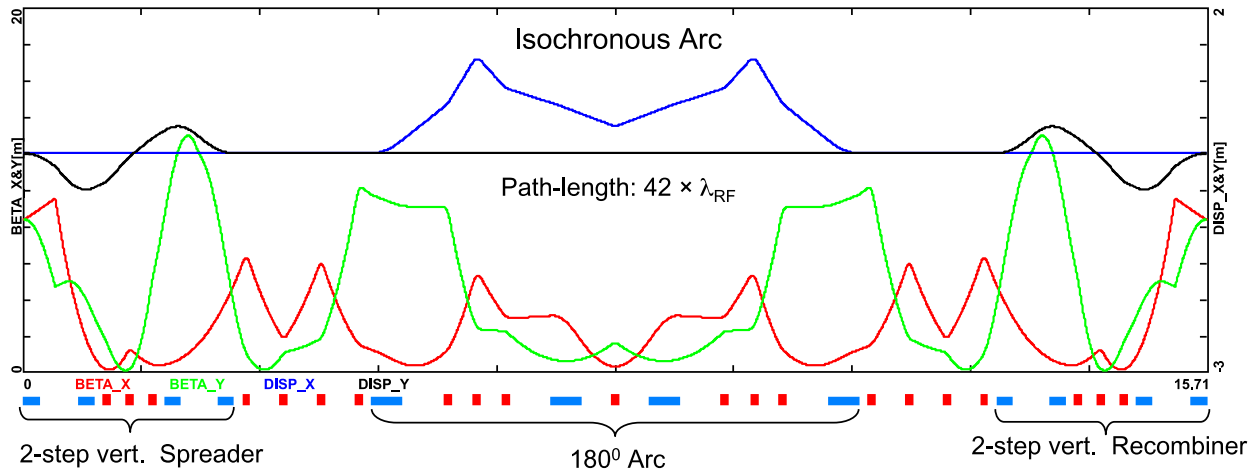


Figure 4: Optics based on the FMC cell for the lowest energy return arc. Horizontal (red curve) and vertical (green curve) beta-function amplitudes are illustrated. Blue and black curves represent the horizontal and vertical dispersion, respectively. The arc, as configured above, is tuned to the isochronous condition ( $M_{56} = 0$ ).

energy arcs (1, 2, 3) are composed of four 45.6 cm long curved  $45^\circ$  bends and of a series of quadrupoles (two triplets and one singlet), while the higher arcs (4, 5, 6) use ‘double length’, 91.2 cm long, curved bends. The usage of curved bends is dictated by a large bending angle ( $45^\circ$ ). If rectangular bends were used, their edge focusing would have caused significant imbalance of focusing, which in turn, would have had adverse effect on the overall arc optics. Another reason for using curved bends is to eliminate the problem of magnet sagitta, which would be especially significant for longer, 91 cm, bends. Each arc is followed by a matching section and a recombiner (mirror symmetric to previously described spreader and matching section). As required in case of mirror symmetric linacs, matching conditions described in the previous section, impose a mirror symmetric arc optics (identical betas and sign reversed alphas at the arc ends). A complete lattice for arc 1 at 70.5 MeV, including a spreader,  $180^\circ$  horizontal arcs and a recombiner, is illustrated in Fig. 4. Presented arc optics features high degree of modular functionality to facilitate momentum compaction management, as well as orthogonal tunability for both the beta functions and dispersion.

The path-length of each arc is chosen to be an integer number of RF wavelengths, except for the highest energy pass, arc 6, whose length is longer by half of the RF wavelength (to shift the RF phase from accelerating to decelerating, switching to the energy recovery mode).

## OUTLOOK – FUTURE STUDIES

We are presently launching a vigorous R&D program to develop a Technical Design Report for PERLE at Orsay, within the next year. To achieve this goal, we have tentatively identified the following sequence of accelerator design studies:

- Linear lattice optimization
- Initial magnet specs

- Momentum acceptance and longitudinal match
- End-to-End simulation with synchrotron radiation, CSR micro-bunching (ELEGANT)
- Correction of nonlinear aberrations (geometric & chromatic) with multipole magnets (sext. and oct.)
- RF cavity design and optimization, HOM content
- Multi-pass BBU studies (TDBBU)
- Injection line/chicane design including space-charge studies at injection
- Diagnostics & Instrumentation
- Multi-particle tracking studies of halo formation
- Final magnet specs
- Engineering design

## ACKNOWLEDGEMENT

Useful discussions and conceptual input from: Oliver Brüning, Erk Jensen, Max Klein and Alessandra Valloni at all stages of the accelerator design process are greatly acknowledged.

## REFERENCES

- [1] G. Arduini et al, ‘PERLE: Powerful ERL for Experiments – Conceptual Design Report’ accepted for publication in Journal of Physics G (2017)
- [2] D. Pellegrini, A. Latina, D. Schulte, S.A. Bogacz, ‘Beam-dynamics Driven Design of the LHeC Energy Recovery Linac’, PRST-AB, **18**, 121004 (2015)
- [3] E. Jensen et al, ‘PERLE - a Powerful ERL Facility Concept’, Proceedings of Nuclear Photonics Conference, Monterey, CA (2016)